This latter orbital is doubly occupied in the case of O^{2-}, but in the case of O^- it loses an electron to form O^{2-} and becomes only half-filled:

$$H_3C{:}H(g) + {\cdot}\underset{\cdot\cdot}{\overset{\cdot\cdot}{O}}{:}^- + Mg^{2+} \longrightarrow {:}\underset{\cdot\cdot}{\overset{\cdot\cdot}{O}}{:}H^- + Mg^{2+}{\cdot}CH_3 \longrightarrow \text{dimerization}$$

or

$$H_3C{:}H(g) + {\cdot}\underset{\cdot\cdot}{\overset{\cdot\cdot}{O}}{:}^- \longrightarrow {:}\underset{\cdot\cdot}{\overset{\cdot\cdot}{O}}{:}H^- + {\cdot}CH_3(g) \longrightarrow \text{dimerization}$$

and in either case the activation energy is low.

Heterolytic CH_4 adsorption ($H^\bullet$ on O^-, $^\bullet CH_3$ on Mg^{2+}) is found to be stable relative to the cluster plus $CH_4(g)$, irrespective of the coordination of the Mg^{2+} to which the $^\bullet CH_3$ binds, the most stable configuration being the one in which both fragments are adsorbed on the 3-coordinated corner ions. Homolytic CH_4 adsorption ($H^\bullet$ on O^-, $^\bullet CH_3$ on O^{2-}) is stable only when $^\bullet CH_3$ adsorbes adjacent to a corner Mg^{2+} because only in this case is the cation dangling-bond orbital which takes the promoted electron sufficiently stable. We calculate a low barrier to mobility for $^\bullet CH_3$ on the face Mg^{2+} sites. Considering that the binding energy of $^\bullet CH_3$ on the face Mg^{2+} sites is only ~ 1 eV (see Table V), the calculations favor its desorption at high temperatures, leading to C_2H_6 formation in the gas phase.

A key question still remaining is why MgO produces different reaction products from $^\bullet CH_3$ radicals than does MoO_3. As discussed above, O^- sites on MgO, generated by the presence of the Li^+ dopant, activate CH_4 to form $^\bullet CH_3$ which in turn form C_2H_6 as the principal selective oxidation product. On MoO_3, CH_4 activated by O^- centers is selectively oxidized primarily to CH_3OH and CH_2O.[5,6,13] There are two prima facie explanations that come to mind. Since MoO_3 possesses more labile lattice oxygen than MgO and is more easily reduced, oxygen addition to the methyl fragment might occur on MoO_3, which would lead to the oxygenated products, but not on MgO, where $^\bullet CH_3$ desorption and dimerization takes place. Another factor of potential importance for answering the above question is the distribution of O^- centers at the surfaces of the two oxides. Wang and Lunsford[19] conclude that most of the $[Li^+O^-]$ centers are not on the surface of MgO and suggest there could be an equilibrium of the form

$$[Li^+O^-]\text{bulk} + O^{2-}\text{surface} \rightleftarrows [Li^+O^{2-}]\text{bulk} + O^-\text{surface}$$

so that the low concentration of surface O^- would explain the selectivity toward C_2H_6 and C_2H_4 formation on this oxide. As discussed in a previous paper,[13] $^\bullet CH_3$ can be strongly trapped on O^-, forming methoxy with a strong C–O bond, which would lead to oxygenated products.

Registry No. MgO, 1309-48-4; MeH, 74-82-8; Me, 2229-07-4; H_2, 1333-74-0.

Asymmetric Nitrogen. 67. Geminal Systems. 41. Chiroptical Properties of *N*-Chloro and *N*-Bromo Derivatives of Three-Membered Nitrogen Heterocycles: Aziridines and Diaziridines[1]

G. V. Shustov, G. K. Kadorkina, R. G. Kostyanovsky,* and A. Rauk[2]

Contribution from the Institute of Chemical Physics, Academy of Sciences of the U.S.S.R., Moscow, U.S.S.R., and the Department of Chemistry, The University of Calgary, Calgary, Canada T2N 1N4. *Received July 21, 1987*

Abstract: An experimental and theoretical investigation of the chiroptical properties of *N*-haloaziridines and -diaziridines is described. The following compounds were synthesized and measured: (1*R*,2*S*)- and (1*S*,2*S*)-1-chloro-2-methylaziridine (**1a** and **1b**), the 2,2-dimethyl analogue (+)-(*S*)-**2**, the methyl esters of (1*R*,2*S*)-1-chloro- and (1*R*,2*S*)-1-bromoaziridine-2-carboxylic acid (**3** and **4**), (1*R*,5*S*,6*R*)-*exo*-6-chloro-5-methyl-1,6-diazabicyclo[3.1.0]hexane (**5**), *endo*- and *exo*-6-chloro-5-trifluoromethyl-1,6-diazabicyclo[3.1.0]hexane (**6a** and **6b**), (1*R*,5*R*,6*S*)-*endo*- and (1*R*,5*R*,6*R*)-*exo*-6-chloro-1,6-diazabicyclo[3.1.0]hexane-5-carboxylic acid methyl ester (**7a** and **7b**), the 6-bromo analogue of **7b**, namely **8**, and the methylamides of (1*S*,5*S*,6*S*)-*exo*-6-chloro- and -6-bromo-1,6-diazabicyclo[3.1.0]hexane-5-carboxylic acid (**9** and **10**). The geometrics of **1a** and **1b** as well as the parent (1*S*,2*R*)- and (1*S*,2*S*)-1-chlorodiaziridine (**11a** and **11b**) were determined by Hartree–Fock SCF calculations by using a 6-31G* basis set. Excitation energies, oscillator strengths, and optical rotatory strengths were computed directly from CI wave functions for the lower singlet states. The lower electronic transitions of both *N*-chloroaziridines and -diaziridines are to valence states described by π^*_{NCl}–σ^*_{NCl} and n_{NNCl}–σ^*_{NCl}, respectively, where π^*_{NCl} and n_{NNCl} are linear combinations of the nonbonded electrons on the heteroatoms and are the HOMO of the respective systems. The long wavelength Cotton effect (CE) of **1a** and **1b** which differ in configuration at the halogenated nitrogen atom have the same sign, negative. The polar carbomethoxy group of **3** has the opposite effect to a methyl group on the first CE of trans *N*-haloaziridines. Theory predicts that the first CE transition of *N*-chlorodiaziridines will change sign upon inversion of configuration at the nonhalogenated nitrogen atom but not on the configuration of the halogenated nitrogen atom. This result is not observed in comparison of the CD spectra of either **6a**,**6b** or **7a**,**7b**. The theoretical and experimental results can be reconciled if the polar groups (CF_3 or CO_2Me) which are also present interfer in the endo(cis) isomers. The signs of the first CE of all of the exo(trans) *N*-halodiaziridine derivatives agree with the theoretical results on **11b**.

Secondary *N*-halogenamines (R_2N-Hal, Hal = Cl, Br) are readily synthesized; they are characterized by an absorption maximum in the accessible region of the UV spectrum.[3,4] Therefore it is interesting to use a halogenamino group as an asymmetrically disturbed chromophore for studying the stereochemistry of chiral amines by chiroptical methods.[5-11] For usual *N*-halogenamines, a low inversion barrier of the nitrogen atom

---

* Address correspondence to this author at The University of Calgary.

(1) Previous papers in this series: Shustov, G. V.; Denisenko, S. N.; Shibaev, A. Yu.; Puzanov, Yu, V.; Kostyanovsky, R. G. *Khim. Fisica* **1988**, in press. (b) Shustov, G. V.; Denisenko, S. N.; Shibaev, A. Yu.; Puzanov, Yu. V.; Romero Maldonado, I. K. A.; Kostyanovsky, R. G. *Izvest. Akad. Nauk SSSR, Ser. Khim.* **1988**, in press.

0002-7863/88/1510-1719$01.50/0

(for chloramines[12-14] $\Delta G^* = 16$–40 kJ mol^{-1}) necessitates the determination of an equilibrium ratio for the invertomers since fast exchange renders them inseparable. The introduction of a halogenamino group into a strained three-membered ring, however, raises the nitrogen inversion barrier (up to about 115 kJ mol^{-1} in *N*-chloroaziridines[15,16]) to the point that individual invertomers may be separated under normal conditions.[15] In derivatives with nonsymmetric substitution at the C atom in the three-membered ring the inversion equilibrium is, as a rule, almost completely shifted toward one isomer.[15,17]

The excited electronic states and chiroptical properties of simple three-membered ring heterocycles have previously been investigated by theoretical methods.[18] In aziridines, the nitrogen atom in the ring is prochiral but becomes a chirotopic[19] center in the case of asymmetric substitution at one of the ring C atoms. The lower electronically excited states of simple aziridines are all Rydberg states,[18,20] the lowest being n-3s, the second corresponding to one of the n-3p manifold. At least in 2-methylaziridine, theoretical studies[18,21] suggest that the sign of the rotatory strengths of the lower transitions are governed by the configuration at the N atom. The situation is quite different in the case of diaziridines which are chiral in the absence of any further substitution. The lowest electronically excited state is a valence state,[18] π^*_N–σ^*_N, and the next, at least in simple diaziridines, is a Rydberg state, π^*–3s. The chromophore is thus intrinsically asymmetric, and it is not surprising that its chirality dominates the sign of the circular dichroism for the lowest transition and possibly of the next few transitions as well.[18] The lowest transition in (1*R*,2*R*)-diaziridines has a negative Cotton effect.[18,22-24]

There are no previous theoretical or experimental studies of the electronic structures or chiroptical properties of *N*-haloaziridines or *N*-halodiaziridines. The N–X bond and the N–N–X grouping are prochiral and asymmetric chromophores, respectively. This paper is devoted to a combined experimental/theoretical investigation of the chiroptical properties of these chromophores in the asymmetrically perturbing environment provided by the N-halogen-substituted aziridines **1–4** and diaziridines **5–10**. Compounds **1–10** were prepared and measured experimentally. Compounds **1** and **11** were investigated theoretically, the latter serving as models for **5–10**.

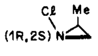

1a

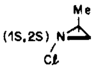

1b

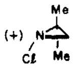

2

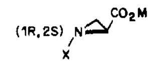

3 X = Cℓ
4 X = Br

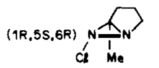

5

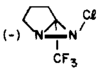

6a

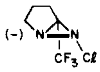

6b

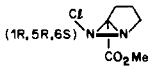

7a

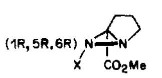

7b X = Cℓ
8 X = Br

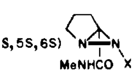

9 X = Cℓ
10 X = Br

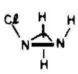

11a

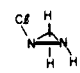

11b

Theoretical Method

The geometries of **1a**, **1b**, **11a**, and **11b** were fully optimized by Hartree–Fock SCF calculations at the 6-31G* level[25] by using the GAUSSIAN 82 system of programs.[26] For the purpose of determining the transition properties, the molecules were recalculated with center-of-mass coordinates by using the 6-31G basis set for C, N, and H. The basis set was augmented by the addition of a single diffuse s function and a set of diffuse p functions (exponent 0.028) to the nitrogen atom. Diffuse functions were not added to the carbon or hydrogen atoms. For the chlorine atom, the 12s,9p atom optimized basis set of Veillard[27] was contracted to 7s,5p by a Raffenetti type contraction scheme.[28] A single set of 3d functions was added (exponent 0.35), as well as a diffuse s function (exponent 0.026) and a set of diffuse p functions (exponent 0.016). The normal 3d polarization functions for C, N, and Cl had to be abandoned for reasons of economy. Addition of the diffuse functions is required in order to describe the lowest few Rydberg states. This basis set is referred to in the tables as the "diffuse" basis to distinguish it from the standard 6-31G* basis.

A brief description of the theoretical method for the determination of oscillator and optical rotatory strengths is given below. A detailed account has been presented elsewhere.[29] Partially correlated wave functions for the ground and excited states are determined to first order in Rayleigh–Schrodinger perturbation theory. Thus

$$\Psi_n = \Psi_n^\circ - \sum_j a_{nj}\Phi_j^\circ \tag{1}$$

where

$$a_{nj} = \langle \Psi_n^\circ : \mathcal{H} : \Phi_j^\circ \rangle / (\langle \Phi_j^\circ : \mathcal{H} : \Phi_j^\circ \rangle - \langle \Psi_n^\circ : \mathcal{H} : \Psi_n^\circ \rangle) \tag{2}$$

$\mathcal{H}$ is the exact Hamiltonian, Φ_j° is a singlet singly or more highly excited configuration derived from the Hartree–Fock determinant Φ_{HF}, and Ψ_n° is a linear combination of quasidegenerate Φ_l° ($l \neq j$) selected from at most singly excited configurations. Thus for the ground state, $\Psi_0^\circ = \Phi_{HF}$. All configurations for which the coefficient a_{nj} (eq 2) was greater than 0.03 were included in the zero-order part of the CI wave function.

Electric dipole transition moments in the length $\langle r \rangle_{on}$ and velocity $\langle v \rangle_{on}$ formalism and magnetic dipole transition moments $\langle m \rangle_{on}$ are explicitly evaluated from

$$\langle r \rangle_{on} = \langle \Psi_o : \vec{\mu} : \Psi_n \rangle \tag{3}$$

$$\langle v \rangle_{on} = \langle \Psi_o : \vec{\nabla} : \Psi_n \rangle / (E_n - E_o) \tag{4}$$

$$\langle m \rangle_{no} = -i \langle \Psi_n : \vec{m} : \Psi_o \rangle \tag{5}$$

---

(2) Department of Chemistry, The University of Calgary, Calgary, Canada T2N 1N4.
(3) Kovacic, P.; Lowery, M. K.; Field, K. W. *Chem. Rev.* **1970**, *70*, 639.
(4) Metcalf, W. S. *J. Chem. Soc.* **1942**, 148–150.
(5) Ripperger, H.; Schreiber, K.; Snatzke, G. *Tetrahedron* **1965**, *21*, 727–732.
(6) Ripperger, H.; Pracejus, H. *Tetrahedron* **1968**, *24*, 99–102.
(7) Ripperger, H.; Schreiber, K. *Tetrahedron* **1969**, *25*, 737–740.
(8) Ripperger, H.; Schreiber, K. *J. Prakt. Chem.* **1971**, *313*, 825–838.
(9) Kostyanovsky, R. G.; Markov, V. I.; Gella, I. M. *Tetrahedron Lett.* **1972**, 1301–1304.
(10) Kostyanovsky, R. G.; Gella, I. M.; Markov, V. I.; Samojlova, Z. E. *Tetrahedron* **1974**, *30*, 39–45.
(11) Shustov, G. V.; Denisenko, S. N.; Chervin, I. I.; Kostyanovsky, R. G. *Izvest. Akad. Nauk SSSR, Ser. Khim.* **1988**, in press.
(12) Rauk, A.; Allen, L. C.; Mislow, K. *Angew. Chem.* **1970**, *82*, 453–468; *Angew. Chem., Int. Ed. Engl.* **1970**, *9*, 400–414.
(13) Lehn, J. M. *Top. Curr. Chem.* **1970**, *15*, 311–377.
(14) Lambert, J. B. *Top. Stereochem.* **1971**, *6*, 19–105.
(15) Kostyanovsky, R. G.; Samojlova, Z. E.; Tchervin, I. I. *Tetrahedron Lett.* **1969**, 719–722.
(16) Kostyanovsky, R. G.; Kadorkina, G. K. *Izvest. Akad. Nauk SSSR Ser. Khim.* **1977**, 1686.
(17) Denisenko, S. N.; Shustov, G. V.; Kostyanovsky, R. G. *J. Chem. Soc., Chem. Commun.* **1983**, 1275–1276; **1985**, 680.
(18) Rauk, A. *J. Am. Chem. Soc.* **1981**, *103*, 1023–1030.
(19) Mislow, K.; Siegel, J. *J. Am. Chem. Soc.* **1984**, *106*, 3319–3328.
(20) Robin, M. B. *Higher Excited States of Polyatomic Molecules*; Academic Press: New York, 1974; Vol. 1, pp 220–222.
(21) Gottarelli, G.; Samori, B.; Bendazzoli, G. L.; Palmieri, P.; Drake, A. F. *Chem. Phys. Lett.* **1977**, *45*, 318–321.
(22) Dyachenko, O. A.; Atovmyan, L. O.; Aldoshin, S. M.; Polyakov, A. E.; Kostyanovsky, R. G. *J. Chem. Soc., Chem. Commun.* **1976**, 50.
(23) (a) Shustov, G. V.; Dyachenko, O. A.; Aldoshin, S. M.; Zolotoi, A. B.; Isobaev, M. D.; Chervin, I. I.; Atovmyan, L. O.; Kostyanovsky, R. G. *Dokl. Akad. Nauk SSSR* **1976**, *231*, 1174–1177. (b) Kostyanovsky, R. G.; Polyakov, A. E.; Shustov, G. V. *Tetrahedron Lett.* **1976**, 2059–2060. (c) Kostyanovsky, R. G.; Shustov, G. V. *Dokl. Akad. Nauk SSSR* **1977**, *232*, 1081–1084. (d) Shustov, G. V.; Denisenko, S. N.; Shokhen, M. A.; Kostyanovsky, R. G. *Izvest. Akad. Nauk SSSR. Ser. Khim.* **1988**, in press.
(24) Haekli, H.; Mannschreck, A. *Angew. Chem.* **1977**, *89*, 419.
(25) (a) Hehre, W. J.; Ditchfield, R.; Pople, J. A. *J. Chem. Phys.* **1972**, *56*, 2257. (b) Hariharan, P. C.; Pople, J. A. *Theor. Chim. Acta* **1973**, *28*, 213.
(26) Binkley, J. S.; Frisch, M. J.; DeFrees, D. J.; Raghavachari, K.; Whiteside, R. A.; Schlegel, H. B.; Fluder, E. M.; Pople, J. A. Department of Chemistry, Carnegie-Mellon University: Pittsburgh, PA.
(27) Veillard, A. *Theor. Chim. Acta* **1968**, *12*, 405–411.
(28) Raffenetti, R. C. *J. Chem. Phys.* **1973**, *58*, 4452–4458. Details of the chlorine atom basis set are available from one of the authors (A.R.).
(29) Rauk, A.; Barriel, J. M. *Chem. Phys.* **1977**, *25*, 409–424.

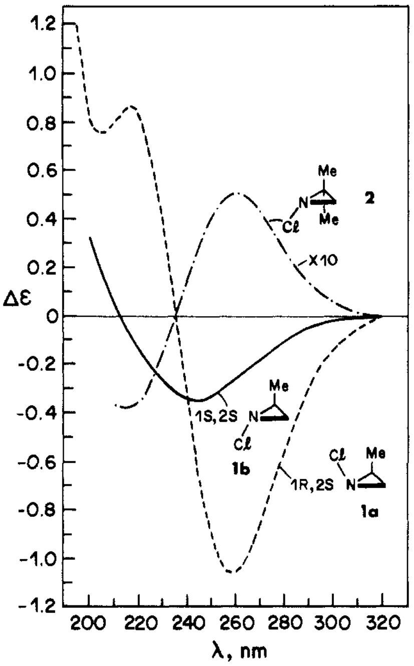

Figure 1. The CD spectra of *N*-chloroaziridines **1a**, **1b**, and **2** in heptane.

where the operators, $\vec{\mu}$, $\vec{\nabla}$, and $\vec{m}$ have their usual definitions[29] and

$$E_n = \langle \Psi_n : \mathcal{H} : \Psi_n \rangle \tag{6}$$

Oscillator strengths f_{on} are calculated by the "mixed" formalism

$$f_{on} = (2/3)\langle \Psi_o : \vec{\nabla} : \Psi_n \rangle \cdot \langle r \rangle_{no} \tag{7}$$

Optical rotatory strengths are evaluated as

$$[R_{on}]^r = \langle r \rangle_{on} \cdot \langle m \rangle_{no} \tag{8}$$

and in the origin-independent form

$$[R_{on}]^v = \langle v \rangle_{on} \cdot \langle m \rangle_{no} \tag{9}$$

The extent of deviation of $\langle r \rangle$ and $\langle v \rangle$ from colinearity and in magnitude is a measure of the quality of the wave functions and origin dependence of $[R]^r$.

Experimental Section

The CD spectra were measured on a JASCO J-500A spectropolarimeter with a DP-500N data processor, the NMR spectra on a Bruker WP-80-SY spectrometer (^{1}H, 80 MHz, from HMDS; ^{13}C, 20.15 MHz, from TMS), and the optical rotation angles on a polarimeter Polamat A.

Cis and trans isomers of 1-chloro-2-methylaziridine **1** were prepared as a 1:1.3 mixture by the action of NaOCl on (2*S*)-2-methylaziridine[30] as previously described.[10] The isomers were separated on a Perkin-Elmer F-21 gas chromatograph (stationary phase XE-52, column 4.5 × 9 mm) at 50 °C: **(1*R*,2*S*)-1-chloro-2-methylaziridine (1a)** $[\alpha]_D^{20}$ −78.2° (*c* 3.3 heptane) and **(1*S*,2*S*)-1-chloro-2-methylaziridine (1b)** $[\alpha]_D^{20}$ +103.4° (*c* 3 heptane). **(+)-1-Chloro-2,2-dimethylaziridine (2)**, $[\alpha]_D^{20}$ +4.5° (*c* 2.8 heptane), was prepared as previously described.[16] The CD spectra of **1** and **2** are shown in Figure 1.

(1*R*,2*S*)-1-Chloroaziridine-2-carboxylic acid methyl ester (3), $[\alpha]_D^{20}$ −193.8° (*c* 2.7 MeOH), was prepared by chlorination of the corresponding (2*S*)-NH-aziridine as described.[11]

(1*R*,2*S*)-1-Bromoaziridine-2-carboxylic Acid Methyl Ester (4). *N*-Bromosuccinimide (0.712 g, 4 mmol) was added to a solution (0.303 g, 3 mmol) of (2*S*)-aziridine-2-carboxylic acid methyl ester[11] in 5 mL of absolute CH_2Cl_2 at 10 °C upon stirring. After having been stirred for 1 h at 20 °C, the solvent was evaporated in vacuo, and the product was extracted from the residue with hexane. After removal of hexane, 0.51 g (94%) of *N*-bromoaziridine **4** was obtained: $[\alpha]_D^{20}$ −232.5° (*c* 2.3 MeOH). The product was identified by ^{1}H NMR and CD spectra (Figure 2, Table I): ^{1}H NMR spectrum in $CDCl_3$ δ, ppm (*J*, Hz): 2.31 (H_B, J_{AB} = 2.7, J_{BC}^{cis} = 7.6), 2.42 (H_A, J_{AC}^{trans} = 4.8), 2.84 (H_C), 3.69 (MeO).

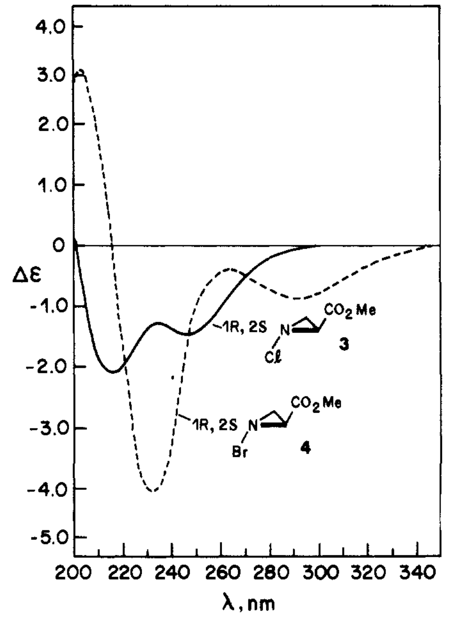

Figure 2. The CD spectra of 1-haloaziridine-2-carboxylic esters **3** and **4** in heptane.

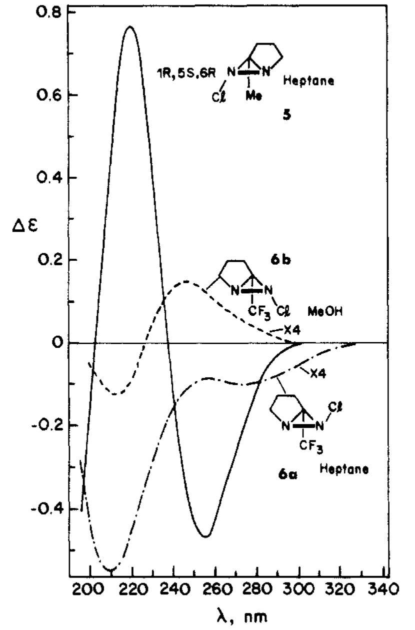

Figure 3. The CD spectra of *N*-chlorodiaziridines **5**, **6a**, and **6b**.

Optically active *N*-halodiaziridines (**5**–**10** have ^{1}H and ^{13}C NMR spectra identical with those of the racemic compounds whose synthesis by the action of *t*-BuOCl and $PyHBr_3$ on the corresponding NH-diaziridines has been described.[17,31,32]

(1*R*,5*S*,6*R*)-*exo*-6-Chloro-5-methyl-1,6-diazabicyclo[3.1.0]hexane (5) with $[\alpha]_D^{20}$ −11.7° (*c* 1.7 heptane) was obtained from (1R,5*S*,6*R*)-5-methyl-1,6-diazabicyclo[3.1.0]hexane, $[\alpha]_D^{20}$ +37.9° (*c* 2.7 heptane), optical purity 75%.[33]

(−)-*endo*-6-Chloro-5-trifluoromethyl-1,6-diazabicyclo[3.1.0]hexane (6a) with $[\alpha]_D^{20}$ −1.3° (*c* 1.4 heptane) was obtained from (−)-5-trifluoromethyl-1,6-diazabicyclo[3.1.0]hexane,[23d] $[\alpha]_D^{20}$ −1.7° (*c* 7.1 hep-

---

(30) Minoura, Y.; Takebayashi, M. *J. Am. Chem. Soc.* **1959**, *81*, 4689–4692.

(31) Shustov, G. V.; Denisenko, S. N.; Kostyanovsky, R. G. *Izvest. Akad. Nauk SSSR, Ser. Khim.* **1983**, 1930–1931.

(32) Shustov, G. V.; Denisenko, S. N.; Chervin, I. I.; Zolotoi, A. B.; D'yachenko, O. A.; Konovalikhin, S. V.; Shilov, G. V.; Atovmyan, L. O.; Kostyanovsky, R. G. *Khim. Geterocikl. Soed.* **1986**, 1330–1336.

(33) Shustov, G. V.; Denisenko, S. N.; Zolotoi, A. B.; D'yachenko, O. A.; Atovmyan, L. O.; Kostyanovsky, R. G. *Izvest. Akad. Nauk SSSR, Ser. Khim.* **1986**, 2266–2271.

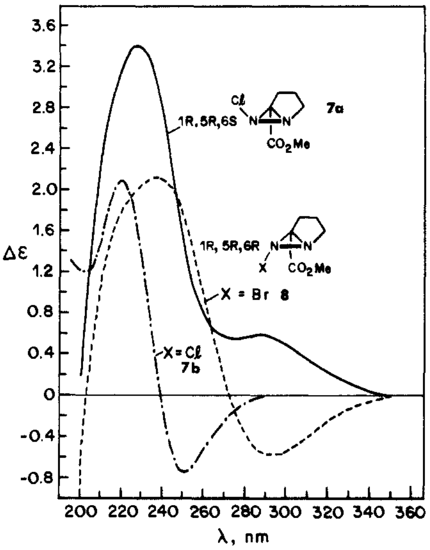

Figure 4. The CD spectra of *N*-halodiaziridines **7a**, **7b**, and **8** in heptane.

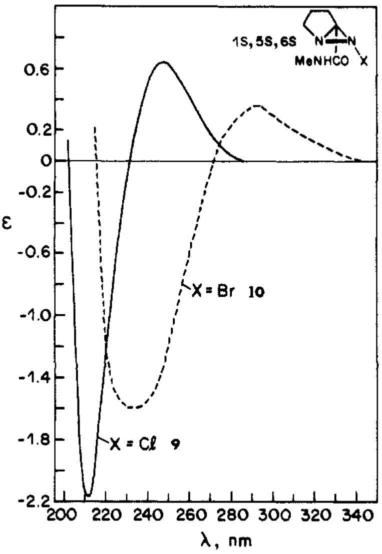

Figure 5. The CD spectra of *N*-halodiaziridines **9** and **10** in MeOH.

tane); *endo*-**6a** transforms quantitatively to ***exo*-6-chloro-5-trifluoromethyl-1,6-diazabicyclo[3.1.0]hexane (6b)** with $[\alpha]_D^{20}$ −0.7° (*c* 2.5 MeOH) upon keeping in MeOH at 20 °C for 1 h. The CD spectra of **5** and **6** are shown in Figure 3.

(1*R*,5*R*,6*S*)-*endo*-6-Chloro-1,6-diazabicyclo[3.1.0]hexane-5-carboxylic acid methyl ester (7a) was obtained from (1*R*,5*R*,6*R*)-1,6-diazabicyclo[3.1.0]hexane-5-carboxylic acid methyl ester, $[\alpha]_D^{20}$ +40.5° (*c* 1.7 MeOH), optical purity 66.5%[33] and identified by ^{13}C NMR[17] and CD spectra (Table I) ; *endo*-*cis*-**7a** transforms quantitatively into **(1*R*,5*R*,6*R*)-*exo*-6-chloro-1,6-diazabicyclo[3.1.0]hexane-5-carboxylic acid methyl ester (7b)** with $[\alpha]_D^{20}$ +6.6° (*c* 1.7 MeOH) at 20 °C.[17] The CD spectra of **7** are given in Figure 4.

(1*R*,5*R*,6*R*)-*exo*-6-Bromo-1,6-diazabicyclo[3.1.0]hexane-5-carboxylic acid methyl ester (8) with $[\alpha]_D^{20}$ +3.7° (*c* 4.4 MeOH) was prepared from (1*R*,5*R*,6*R*)-1,6-diazabicyclo[3.1.0]hexane-5-carboxylic acid methyl ester, $[\alpha]_D^{20}$ +40.5° (*c* 1.7 MeOH), optical purity 66.5%.[33] See Figure 4 for the CD spectrum of **8**.

Methylamides of (1*S*,5*S*,6*S*)-*exo*-6-chloro- and 6-bromo-1,6-diazabicyclo[3.1.0]hexane-5-carboxylic acid (9 and 10) with $[\alpha]_D^{20}$ −34.4° (*c* 1.4 MeOH) and −25.7° (*c* 0.7 MeOH), respectively, were synthesized from methylamide of (1*S*,5*S*,6*S*)-1,6-diazabicyclo[3.1.0]hexane-5-carboxylic acid, $[\alpha]_D^{20}$ −55.8° (*c* 1.2 MeOH), optical purity 78%.[33] The CD spectra of **9** and **10** are presented in Figure 5.

Results and Discussion

***N*-Haloaziridines 1–4. Experimental.** The absolute configurations of the *N*-haloaziridines **1**, **3**, and **4** follow from the configurations of the corresponding NH-aziridines, synthesized from natural amino acids (*S*)-alanine[10] and (*S*)-serine.[11]

Table I. Experimental CD Spectra of *N*-Haloaziridines **1–4** and *N*-Halodiaziridines **5–10**[a]

	band I		band II		
compd	λ_{max} (nm)	Δε	λ_{max} (nm)	Δε	solvent
1a	260	−1.060	216	+0.867	heptane
	259	−0.885	215	+0.852	MeOH
1b	244	−0.354			heptane
	237	−0.295			MeOH
2	260	+0.051	217	−0.038	heptane
3	247	−1.470	216	−2.103	heptane
	245	−1.410	215	−1.952	MeOH
4[b]	293	−0.879	232	−4.181	heptane
	281	−0.970	229	−3.515	MeOH
5	255	−0.468	220	+0.767	heptane
6a	273	−0.025	209	−0.137	heptane
6b	247	+0.038	213	−0.031	MeOH
7a	288	+0.597	228	+3.310	heptane
	287	+0.577	227	+2.155	MeCN
			212	+2.463	
7b	251	−0.751	220	+2.098	heptane
	251	−0.616	220	+1.732	MeCN
	250	−0.732	218	+2.216	MeOH
8	293	−0.564	236	+2.137	heptane
	289	−0.504	233	+1.601	MeOH
			217	+1.848	
9	248	+0.632	213	−2.176	MeOH
10	291	+0.363	233	−1.606	MeOH

[a] For compounds **5** and **7–10** the values of Δε are recalculated with respect to 100% optical purity. [b] Band III, λ_{max} (Δε): 203 (+3.08) in heptane; 203 (+2.606) in MeOH.

In the CD spectrum of both isomers of 1-chloro-2-methylaziridine, (1*R*,5*S*)-**1a** and (1*S*, 2*S*)-**1b**, a negative long wavelength (first) Cotton effect (CE) is observed (Figure 1, Table I). The magnitude of this effect for the cis isomer **1a** exceeds 3 times that for the trans isomer **1b**, suggesting a greater asymmetric disturbance of the chloramine chromophore by the α-cis methyl group.

In accordance with the relative contributions of cis and trans Me groups to the long wavelength CE of *N*-chloroaziridine, the absolute configuration of the product of asymmetric synthesis, (+)-1-choro-2,2-dimethylaziridine (**2**)[16] should be assigned (1*S*) on the basis of it having a positive CE at 260 nm Figure 1, Table I). This corrects the earlier misassignment[16] on the basis of the octant rule.[9] Almost a complete coincidence of both dichroic absorbance bands of (+)-**2** and (1*R*,2*S*)-*cis*-**1a** confirms the decisive influence of the cis Me group on the CD spectrum of *N*-chloroaziridine **2** (Figure 1, Table I). A long wavelength shift of the first CE (by 16 nm) in *cis*-**1a** and the 2,2-dimethyl derivative **2** may be due to steric interaction of the Cl atom and the cis Me group; as a result of the interaction, the nitrogen pyramid is flattened with consequent raising of the highest occupied molecular orbital (HOMO), the antibonding combination of the lone pairs on nitrogen and chlorine, and narrowing of the HOMO–LUMO gap.

N-Chloroaziridine **3**, like **1b**, has a group trans to the chlorine. In the CD spectrum of **3** (Figure 2, Table I) the position of the

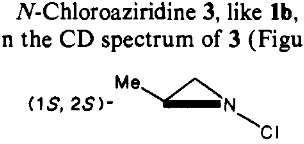

1b: $-\Delta\varepsilon_{244}$

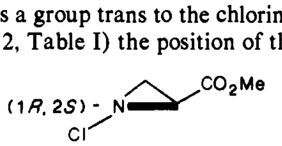

3: $-\Delta\varepsilon_{247}$

first band and its sign are the same as for **1b** although the configurations at each chiral center are reversed, (1*R*,2*S*)-**3** versus (1*S*,2*S*)-**1b**. While the dichroic absorbances of the carbomethoxy group do overlap the first chloramine band, inspection of the CD spectrum of the *N*-bromoaziridine (1*R*,2*S*)-**4** (Figure 2) reveals that the stronger ester absorption is not masking a weaker chloramine absorption of opposite sign. In **4** the *N*-halamine absorption is shifted to longer wavelength but still has the same sign. It appears that the asymmetric disturbance of the *N*-halamine chromophore by the trans oriented ester and methyl group is of opposite sign.

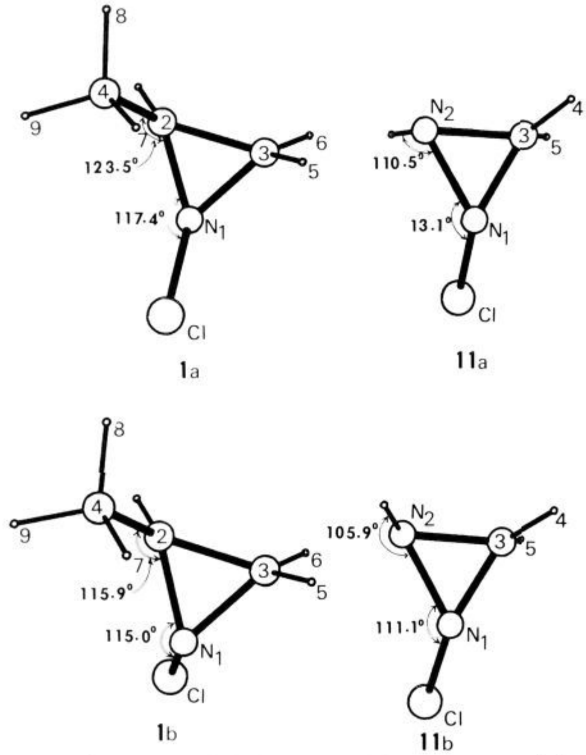

Figure 6. Structures optimized at the 6-31G* level (bond lengths in Å, bond angles in deg): **1a** N_1–Cl, 1.730; N_1–C_2, 1.459; N_1–C_3, 1.452; C_2–C_3, 1.475; C_2–H, 1.077; C_2–C_4, 1.509; C_3–H_5, 1.075; C_3–H_6; 1.075; C_4–H_7, 1.081; C_4–H_8, 1.085; C_4–H_9, 1.084; C_2N_1Cl, 117.4; C_3N_1Cl, 115.6; N_1C_2H, 109.8; C_3C_2H, 117.6; $N_1C_2C_4$, 123.5; $C_3C_2C_4$, 121.9; $N_1C_3H_5$, 114.2; $C_2C_3H_5$, 117.1; $N_1C_3H_6$, 117.3; $C_2C_3H_4$, 121.9; $C_2C_4H_7$, 112.4; $C_2C_4H_8$, 108.9; $C_2C_4H_9$, 110.6; $H_7C_4H_8$, 108.3; $H_9C_4H_8$, 108.1; $N_1C_2C_4H_7$, 47.8; **1b** N_1–Cl, 1.731; N_1–C_2, 1.453; N_1–C_3, 1.454; C_2–C_3, 1.474; C_2–H, 1.077; C_2–C_4, 1.507; C_3–H_5, 1.076; C_3–H_6, 1.075; C_4–H_7, 1.083; C_4–H_8, 1.086; C_4–H_9, 1.085; C_2N_1Cl, 115.0; C_3N_1Cl, 114.6; N_1C_2H, 115.4; C_3C_2H, 115.1; $N_1C_2C_4$, 115.9; $C_3C_2C_4$, 123.3; $N_1C_3H_5$, 113.8; $C_2C_3H_5$, 121.0; $N_1C_3H_6$, 117.6; $C_2C_3H_6$, 118.0; $C_2C_4H_7$, 110.8; $C_2C_4H_8$, 108.2; $C_2C_4H_9$, 110.6; $H_7C_4H_8$, 108.2; $H_9C_4H_8$, 108.3; $N_1C_2C_4H_7$, 39.1; **11a** N_1–Cl, 1.746; N_1–N_2, 1.440; N_1–C_3, 1.433; N_2–C_3, 1.423; N_2–H, 1.003; C_3–H_4, 1.074; C_3–H_5, 1.074; N_2N_1Cl, 113.1; C_3N_1Cl, 112.0; N_1N_2H, 110.5; C_3N_2H, 111.3; $N_1C_3H_4$, 115.4; $N_2C_3H_4$, 116.5; $N_1C_3H_5$, 117.5; $N_2C_3H_5$, 119.4; **11b** N_1–Cl, 1.732; N_1–N_2, 1.431; N_1–C_3, 1.427; N_2–C_3, 1.421; N_2–H, 1.003; C_3–H_4, 1.076; C_3–H_5, 1.074; N_2N_1Cl, 111.1; C_3N_1Cl, 114.5; N_1N_2H, 105.9; C_3N_2H, 113.0; $N_1C_3H_4$, 114.4; $N_2C_3H_4$, 120.7; $N_1C_3H_5$, 118.8; $N_2C_3H_5$, 115.1.

A small blue shift of the first CE in the CD spectra of the *N*-halogenaziridines, **1**, **3**, and **4**, when heptane is substituted for methanol (Table I), supports the participation of nonbonding electrons in the optically active transition.

Theoretical. The geometries of **1a** and **1b** optimized with the 6-31G* basis set are shown in Figure 6. The SCF energies of **1a** and **1b** are given in Table II. At the SCF level, the cis isomer is about 10 kJ mol^{-1} less stable than the trans. The buttressing effect of the methyl group is seen by comparing the two structures (Figure 6). In **1a**, the N_1–C_2 bond is slightly longer, the C_2–N_1–Cl angle is 2.4° larger, and the N_1–C_2–C(Me) angle is 7.6° larger than the corresponding parameters of **1b**. Evidently, there is more flexibility to respond to the steric interaction at the C atom in the ring than at the N atom.

The molecular orbitals involved in the electronic transitions discussed below are shown in Figure 7. The HOMO of each of **1a** and **1b** is largely an antibonding combination of the lone pairs of the N and Cl atoms with a significant admixture of one of the Walsh-type orbitals which describes the bonding of the strained three-membered ring. We shall refer to this orbital as π^*_{NCl}. The longest wavelength electronic transition originates from this orbital. The second highest molecular orbital of both compounds is mainly a 3p nonbonding orbital on chlorine with an out-of-phase admixture of the second Walsh-type 3-ring bonding orbital. The second electronic transition of each compound originates from this orbital which we will call $3p_{Cl}$. The distribution of the "excited" electron (after CI) in both the first and second excited states of each compound is highly localized to the N–Cl bond and is designated σ^*_{NCl}.

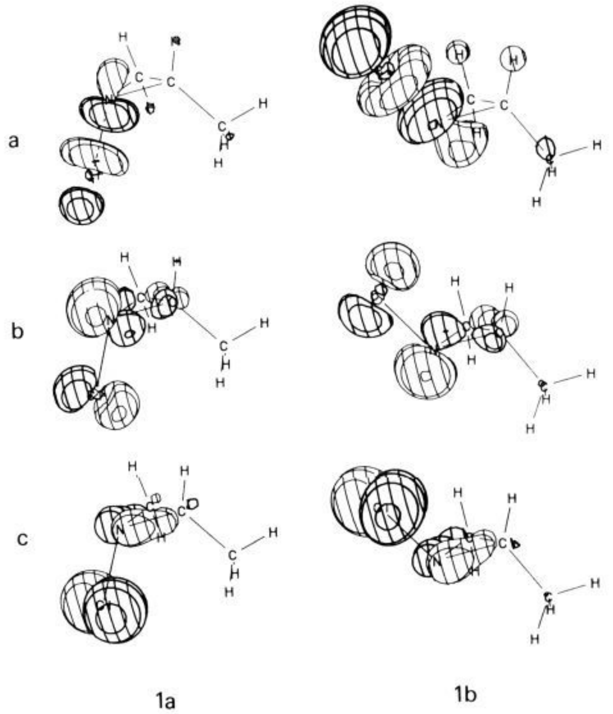

Figure 7. MOs^{35} of **1a** and **1b** at contour 0.075: (a) σ^*_{NCl}, (b) π^*_{NCl} (HOMO), and (c) $3p_{Cl}$. Thick and thin lines denote relative phases.

The derived transition properties of **1a** and **1b** are collected in Table II. The rotatory strength is reported as calculated by both the length ($[R]^r$ eq 3) and velocity ($[R]^v$ eq 4) formalism. The latter is origin-independent, and the agreement between the two serves as a measure of the quality of the wave functions for the two states involved in the transition (the ground state and one of the excited states). The angle between the electric dipole transition moments, expressed in the length and velocity formalism, bears a similar function. The angles between the magnetic dipole transition moment and the electric dipole transition moments in the two formalisms are also quoted in Table II, although discussion of these is meaningful only if the origin is near the center of mass owing to the origin dependence of the magnetic dipole transition moment. Angles near 90° result in very small rotatory strengths which may be subject to subtle influences from the environment that change the local shape of the chromophore. This is the case for the lowest electronic transition, π^*_{NCl}–σ^*_{NCl}, of each compound. However, the signs of the rotatory strength calculated by both methods (i.e., $[R]^v$ and $[R]^r$) agree in sign and are the same as observed in the experimental CD spectrum (Figure 1). Also in agreement with experiment, the lowest transition of **1a** is at longer wavelength than in **1b**, and the rotational strength of the cis isomer is larger than that of the trans, as seen by comparing the $[R]^v$ values in Table II.

The second electronic transitions of each compound also are to valence states and have similar oscillator strengths. In each case, the transition originates from the second highest occupied MO but terminates in the same N–Cl antibonding orbital. In **1b**, the CE of this transition is predicted to be weak and negative. In **1a**, the CE is predicted to be weaker still and of indeterminate sign. Although the angle between $\langle r \rangle$ and $\langle v \rangle$ is calculated to be only 4°, the resulting angles between $\langle r \rangle$ and $\langle m \rangle$ and between $\langle v \rangle$ and $\langle m \rangle$ are on either side of 90°, leading to predictions of opposite sign for the CE. If the origin independent form $[R]^v$ is taken as more reliable, then the sign of the CE of this transition

Table II. Calculated Properties for (1*R*,2*S*)-1-Chloro-2-methylaziridine (**1a**) and (1*S*,2*S*)-1-Chloro-2-methylaziridine (**1b**)[a]

property			**1a**		**1b**	
			6-31G*	diffuse	6-31G*	diffuse
E_{SCF}, hartree			−630.937487	−630.87391	−630.941382	−630.87751
MO energies, eV	π^*_{NCl}	24a	−10.27	−10.25[b]	−10.41	−10.43[b]
	$3p_{\mathrm{Cl}}$	23a	−11.48	−11.53[b]	−11.46	−11.51[b]
		22a	−12.96	−13.00	−12.96	−12.95
		21a	−13.29	−13.34	−13.30	−13.38
		20a	−14.34	−14.35	−14.24	−14.26
μ, D			2.883	3.112	2.774	2.976
$S_0 \rightarrow S_1$	E, eV			5.82		5.95
	$[R]^v$ ($[R]^r$)			−4.0 (−0.7)		−0.5 (−1.8)
	f			0.0244		0.0225
	descriptn[c]			$\pi^*_{\mathrm{NCl}}-\sigma^*_{\mathrm{NCl}}$[b]		$\pi^*_{\mathrm{NCl}}-\sigma^*_{\mathrm{NCl}}$[b]
	$\langle r\rangle,\langle m\rangle,\langle v\rangle$[d]			0.322, 0.096, 0.545		0.306, 0.148, 0.510
	$\langle r\rangle\cdot\langle m\rangle,\langle v\rangle\cdot\langle m\rangle,\langle r\rangle\cdot\langle v\rangle$[e]			95, 107, 12		98, 92, 11
$S_0 \rightarrow S_2$	E, eV			6.96		6.91
	$[R]^v$ ($[R]^r$)			+0.9 (−0.5)		−1.2 (−1.2)
	f			0.0077		0.0055
	descriptn[c]			$3p_{\mathrm{Cl}}-\sigma^*_{\mathrm{NCl}}$[b]		$3p_{\mathrm{Cl}}-\sigma^*_{\mathrm{NCl}}$[b]
	$\langle r\rangle,\langle m\rangle,\langle v\rangle$[d]			0.184, 0.405, 0.245		0.148, 0.486, 0.212
	$\langle r\rangle\cdot\langle m\rangle,\langle v\rangle\cdot\langle m\rangle,\langle r\rangle\cdot\langle v\rangle$[e]			92, 88, 4		94, 93, 1
$S_0 \rightarrow S_3$	E, eV			7.79		8.10
	$[R]^v$ ($[R]^r$)			−0.2 (0.0)		−19.3 (−17.4)
	f			0.0001		0.0133
	descriptn[c]			$\pi^*_{\mathrm{NCl}}-4s_{\mathrm{Cl}}$		$\pi^*_{\mathrm{NCl}}-4s_{\mathrm{Cl}}$
	$\langle r\rangle,\langle m\rangle,\langle v\rangle$[d]			0.056, 0.151, 0.050		0.240, 0.535, 0.279
	$\langle r\rangle\cdot\langle m\rangle,\langle v\rangle\cdot\langle m\rangle,\langle r\rangle\cdot\langle v\rangle$[e]			90, 97, 76		122, 121, 2
$S_0 \rightarrow S_4$	E, eV			8.29		8.34
	$[R]^v$ ($[R]^r$)			15.0 (8.8)		13.7 (11.0)
	f			0.0131		0.0266
	descriptn[c]			$\pi^*_{\mathrm{NCl}}-3d_{\mathrm{Cl}}$		$\pi^*_{\mathrm{NCl}}-3d_{\mathrm{Cl}}$
	$\langle r\rangle,\langle m\rangle,\langle v\rangle$[d]			0.263, 0.550, 0.252		0.379, 0.311, 0.349
	$\langle r\rangle\cdot\langle m\rangle,\langle v\rangle\cdot\langle m\rangle,\langle r\rangle\cdot\langle v\rangle$[e]			76, 65, 14		68, 60, 10

[a] Geometries optimized with 6-31G* basis set (see figure 6). [b] See Figure 7. [c] Each of the excitations originates from a single canonical MO and terminates in an "excited" MO which is a linear combination of canonical virtual MOs. The combined CI coefficient for the excitation from the single MO is >0.96. [d] Magnitudes in atomic units. [e] Angles in deg.

is the same as observed eperimentally, namely positive.

The next higher excited singlet states of both compounds are predicted to be Rydberg states, corresponding to $\sigma^*_{\mathrm{NCl}}-4s_{\mathrm{Cl}}$, and $\pi^*_{\mathrm{NCl}}-3d_{\mathrm{Cl}}$ transitions. The latter are not adequately described within the limitations of the present basis set and are probably calculated to occur at relatively too high energies.

The present calculations do not shed light on the reason that the perturbative effect of the electron-withdrawing carbomethoxy group on the CE of the first electronic transition is opposite to that of the Me group. One may argue that since the CE of **2** as measured by $\Delta\epsilon_{\max}$ is stronger than that of **1b**, the structural unit **12** should be considered to be a chiral chromophore in its own right, with a contribution to the first CE as shown below. This concept gains additional support from the discussion of the *N*-halodiaziridines below in which electronically and structurally similar units recur with X = R and Y = CF$_3$, CO$_2$Me.

(+)-**12** (−)-**12**

X = Cl; Br
Y = CO$_2$R

***N*-Halodiaziridines 5–11. Experimental.** The absolute configuration of the NH-aziridine (+)-5-methyl-1,6-diazabicyclo[3.1.0]hexane, yielding (1*R*,5*S*,6*R*)-**5**, was assigned by comparing the ORD spectrum of this compound with the spectra of other 1,3,3-trialkyldiaziridines;[23d] the absolute configurations of (1*R*,5*R*,6*R*)-(+)-methyl ester and (1*S*,5*S*,6*S*)-(−)-methylamide of 1,6-diazabicyclo[3.1.0]hexane-5-carboxylic acid, precursors to **7** and **8** and **9** and **10**, respectively, were assigned on the basis of X-ray analysis of the 1-epherinium salt of this acid.[33,34] The absolute configuration of the precursor of **6**, (−)-5-trifluoromethyl-1,6-diazabicyclo[3.1.0]hexane, was not determined reliably.[23d]

Inspection of Table I and Figures 3 and 4 reveals that the position of the dichroic absorbance maxima in the CD spectrum is at longer wavelength for the endo(cis) isomers **6a** and **7a** than in the exo(trans) isomers **6b** and **7b**. Endo(cis) and exo(trans) isomers of *N*-chlorodiaziridines **6** and **7** differ also by the sign of the long wavelength CE (Figures 3 and 4, Table I). A comparison of the CD spectra of exo(trans)-*N*-chlorides **5**, **7b**, and **9** shows that contrary to *N*-chloroaziridines **1b** and **3** the substitution of a better electron acceptor and more polar CO$_2$Me (of CONHMe) group for Me leads only to a blue shift, whereas the sign of the long wavelength band of dichroic absorbance remains unchanged. The fact that the sign of the first CE f *N*-chlorodiaziridines **7d** and **9** is not the result of overlapping of the bands of N–N–Cl and ester (or amide) chromophores is confirmed by the CD spectra of the exo(trans) *N*-bromides **8** and **10** (Figures 4 and 5, Table I) whose CE signs are similar to those of the *N*-chloro analogues. The substitution of MeOH for aprotic solvents (heptane, MeCN) results in a blue shift in the CD spectra of the *N*-halogendiaziridines **7b** and **8** as has already been noted for *N*-haloaziridines **1**, **3**, and **4** (Table I).

Theoretical. The geometries of *cis*-(1*S*,2*R*)-1-chlorodiaziridine **11a** and its trans isomer, *trans*-(1*S*,2*S*)-**11b**, are shown in Figure 6. In the cis isomer, the N–N and N–Cl bonds are about 0.01 Å longer than in the trans isomer. The N–Cl bond is tipped about 2° further away from the second nitrogen atom. The N–H bond is bent almost 5° further away from the chlorine in the cis compound. The cis compound **11a** is 19 kJ mol^{-1} less stable than the trans isomer **11b**.

In contrast to the *N*-haloaziridines **1–4**, in the *N*-halodiaziridines, the nature of the chromophore changes completely. It should be considered as the N–N–Cl chromophore in which

---

(34) Zolotoi, A. B.; D'yachenko, O. A.; Atovmyan, L. O.; Shustov, G. V.; Denisenko, S. N.; Kostyanovsky, R. G. *Izvest. Akad. Nauk SSSR, Ser. Khim.* **1986**, 2441–2446.

(35) Jorgensen, W. A. *QCPE* **1977**, *11*, 340.

Table III. Calculated Properties for (1*S*,2*R*)-1-Chlorodiaziridine (**11a**) and (1*S*,2*S*)-1-Chlorodiaziridine (**11b**)[a]

property			**11a**		**11b**	
			6-31G*	diffuse	6-31G*	diffuse
E_{SCF}, hartree			−607.857336	−607.78573	−607.864584	−607.79295
MO energies, eV	n_{NNCl}	20a	−10.87	−10.95[b]	−11.14	−11.20[b]
	$3p_{Cl}$	19a	−11.95	−12.05[b]	−11.86	−11.96[b]
		18a	−13.12	−13.26	−12.22	−12.31
		17a	−14.40	−14.48	−13.99	−14.12
		16a	−15.07	−15.26	−15.06	−15.20
μ, D			2.962	3.297	2.941	3.103
$S_0 \rightarrow S_1$	E, eV			5.85		6.29
	$[R]^v$ ($[R]^r$)			−8.1 (−9.9)		9.1 (5.3)
	f			0.0367		0.0267
	descriptn[c]			$0.90(n_{NNCl}-\sigma^*_{NCl}{}^b)$		$0.92(n_{NNCl}-\sigma^*_{NCl}{}^b)$
	$\langle r\rangle,\langle m\rangle,\langle v\rangle^d$			0.441, 0.193, 0.594		0.336, 0.248, 0.548
	$\langle r\rangle\cdot\langle m\rangle,\langle v\rangle\cdot\langle m\rangle,\langle r\rangle\cdot\langle v\rangle^e$			117, 106, 12		76, 75, 20
$S_0 \rightarrow S_2$	E, eV			6.99		6.99
	$[R]^b$ ($[R]^r$)			0.2 (0.7)		−2.7 (+1.0)
	f			0.0032		0.0047
	descriptn[c]			$0.89(3p_{Cl}-\sigma^*_{NCl}{}^b)$		$0.75(3p_{Cl}-\sigma^*_{NCl}{}^b)$
	$\langle r\rangle,\langle m\rangle,\langle v\rangle^d$			0.096, 0.639, 0.196		0.116, 0.527, 0.244
	$\langle r\rangle\cdot\langle m\rangle,\langle v\rangle\cdot\langle m\rangle,\langle r\rangle\cdot\langle v\rangle^e$			87, 89.6, 12		86, 95, 11
$S_0 \rightarrow S_3$	E, eV			7.83		8.24
	$[R]^v$ ($[R]^r$)			−18.1 (−16.4)		5.1 (7.2)
	f			0.0248		0.0085
	descriptn[c]			$0.92(n_{NNCl}-4s_{Cl})$		$0.68(n_{NNCl}-4s_{Cl})$
	$\langle r\rangle,\langle m\rangle,\langle v\rangle^d$			0.337, 0.327, 0.384		0.168, 0.386, 0.260
	$\langle r\rangle\cdot\langle m\rangle,\langle v\rangle\cdot\langle m\rangle,\langle r\rangle\cdot\langle v\rangle^e$			126, 125, 5		64, 78, 16
$S_0 \rightarrow S_4$	E, eV			8.08		8.42
	$[R]^v$ ($[R]^r$)			−38.0 (−28.2)		12.4 (11.6)
	f			0.0431		0.0222
	descriptn[c]			$0.68(18a-\sigma^*_{NCl})$		$0.60(n_{NNCl}-3d_{Cl})$
	$\langle r\rangle,\langle m\rangle,\langle v\rangle^d$			0.461, 1.106, 0.478		0.324, 0.225, 0.335
	$\langle r\rangle\cdot\langle m\rangle,\langle v\rangle\cdot\langle m\rangle,\langle r\rangle\cdot\langle v\rangle^e$			103, 106, 9		51, 50, 8

[a] Geometries optimized with 6-31G* basis set (see Figure 6). [b] See Figure 8. [c] Each of the excitations terminates in an "excited" MO which is a linear combination of canonical virtual MOs. Minor CI components >0.05: **11a** S_1, 0.07 (18a→..); S_2, 0.08 (18a→..); S_4, 0.23 (n_{NNCl}→..), 0.06 ($3p_{Cl}$→..); **11b** S_2, 0.25 (18a→..); S_3, 0.11 ($3p_{Cl}$→..), 0.20 (18a→..); S_4, 0.11 ($3p_{Cl}$→..), 0.27 (18a→..). [d] Magnitudes in atomic units. [e] Angles in deg.

the higher occupied molecular orbitals are linear combinations of the nonbonding electron pairs on all three heteroatoms as shown for the parent molecules **11a** and **11b** as Figure 8. There are also differences to be noted between the two isomeric structures. In **11a** the HOMO is essentially the out-of-phase combination of the nonbonded electron pairs of the two nitrogen atoms with some admixture of one of the nonbonded electron pairs of the chlorine atom and of a ring bonding orbital. By contrast, the HOMO of *trans*-**11b** is weighted more toward the chlorine atom with relatively little contribution from N_2 and none from the ring orbitals. A major difference between the HOMOs of **11a** and **11b** occurs at N_2 with respect to the orientation of the hybridized atomic orbital component. For simplicity we denote the HOMO of each as n_{NNCl}. As seen in Table III, the HOMO of **11a** is almost 0.3 eV higher in energy than the HOMO of **11b**.

The second highest occupied orbitals (MO 19a) exhibit greater differences, particularly in the orientation of the nonbonded electron pairs on chlorine (Figure 8) although they are similar in energy (Table III). In **11a**, this orbital is out of phase with the smaller in-phase combination of the nonbonded orbitals of the nitrogen atoms. In **11b**, the chlorine 3p orbital is out of phase with a ring bonding orbital and as a result is rotated by almost 90° relative to the $3p_{Cl}$ component of MO 19a of **11a**. In recognition of the major contribution from the chlorine atom to MO 19a, this orbital is designated as $3p_{Cl}$ as was the case in **1a** and **1b**.

The first two electronic transitions are calculated in the case of the parent system **11a** and **11b** to originate from each of the two highest occupied orbitals in turn. The distribution of the "excited" electron in each case is a highly localized axially symmetric σ^*_{NCl} as was the case in the *N*-haloaziridines. The terminal orbital of the first transition of **11a** and **11b** is shown in Figure 8. The terminal orbital of the second transition is visually indistinguishable and is not shown.

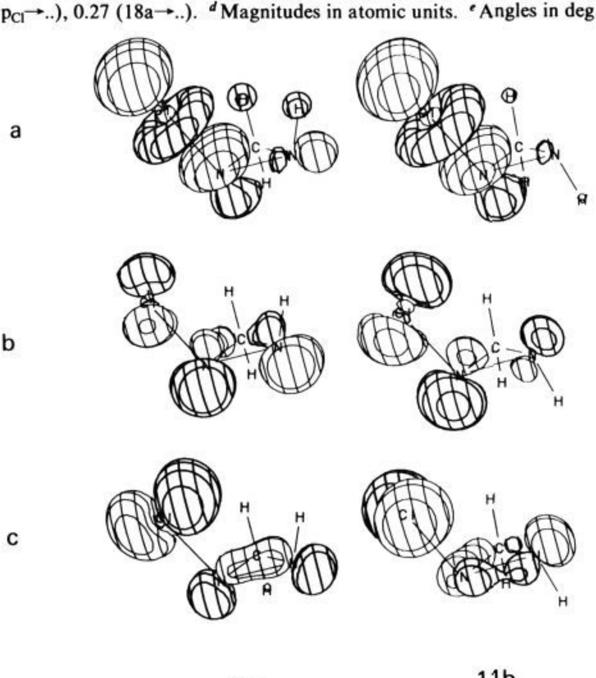

Figure 8. MOs[35] of **11a** and **11b** at contour 0.075: (a) σ^*_{NCl}, (b) n_{NNCl} (HOMO), and (c) $3p_{Cl}$. Thick and thin lines denote relative phases.

The calculated transition properties of **11a** and **11b** are collected in Table III. The signs of the CE of the first transition $n_{NNCl}-\sigma^*_{NCl}$ of (1*S*,2*R*)-**11a** and (1*S*,2*S*)-**11b** are calculated to be negative and positive, respectively. Thus the CE of the first transition of the NNCl three-ring chromophore is predicted to *change sign upon inversion at N_2 but not at N_1*. At first glance, the experimental data on compounds **5**–**10** do not support this theoretical result. While the sign of the first CE of all of the *trans-N*-halodiaziridines **5**, **6b**, **7b**, and **8**–**10** are as expected from the calculated result for **11b**, neither of the cis analogues, **6a** nor **7a**, has a CE as predicted on the basis of **11a** as model. We return to this point below. The observed red shifts in the first transition of the cis isomers relative to the trans isomers, 0.48 and 0.62 eV for **6** and **7**, respectively, correspond well with that calculated for **11**, namely 0.44 eV.

The second electronic transition of **11a** and **11b** is calculated to have a much lower dipole strength than the first (Table III) and is predicted to originate from the second highest occupied MO but to terminate in the same antibonding orbital, namely $3p_{Cl}-\sigma^*_{NCl}$. No isomer red shift is expected for this transition. The calculated separation of the two transitions in *trans*-**11b**, 0.7 eV, is the same as observed in the case of **5** (Table III). The electric and magnetic dipole transition moments are very nearly orthogonal in **11a** and **11b**. On this basis one expects the sign and magnitude of the CE of this transition to be dependent on the intramolecular and extramolecular environment of the chromophore. In compounds **5**, **6a**, and **6b** the signs observed for the CE of the second transition (Table I, Figure 3) are as calculated by the origin-independent form of the rotational strength, $[R]^V$. The ester and amide groups of **7**–**10** also absorb in the region of the second *N*-halodiaziridine band precluding direct comparison with computed results for **11** for this transition.

We return to the question of the discrepancy between the experimental observations on compounds **6** and **7** from which one may conclude that the first CE of *N*-chlorodiaziridines changes sign upon inversion of configuration at the halogenated nitrogen and the theoretical results from **11** that predict that the decisive configuration is at the non-halogenated nitrogen atom. whether the discrepancy is real or not hinges on how good a model **11** is for the *N*-halodiaziridines **5**–**10**. The most serious objection to the use of **11** as a model is the presence of the highly polar substituent (CF_3, CO_2Me, or CONHMe) at the C position of the diaziridine ring (position 5 of the 1,6-diazabicyclo[3.1.0]hexane skeleton) which is present in all compounds except **5** which has a more innocuous Me group at this position. The computed results for **11b** should be most comparable to the experimental observations on compound **5** and indeed agree in all important details. Extrapolating the computed results for **11a** to the *cis* isomer of **5**, namely **13**, the theory predicts that the sign of the first CE of **13** is negative as it is in the case of **5**. Extrapolation from the experimental results for **6** and **7** suggests that the first CE of **13** should be positive. The discrepancy may be resolved if one assumes that the chiral moiety **12** which is also present in the diaziridines does not play a benign role as one may suppose from the CD spectra of **6** and **7** (Figures 3 and 4) but rather a dominant role, reversing the sign of the first CE of the cis *N*-halodiaziridines, in the same manner as in the case of *N*-haloaziridines (compare **3** and **4** with **1b**, Figures 1 and 2.) Unfortunately, in contrast to the *N*-chlorodiaziridines **6a** and **7a**, low configurational stability of **13** does not allow the synthesis of this compound by chlorination of 5-methyl-1,6-diazabicyclo[3.1.0]hexane.[1a,31] In addition, direct computation on systems the size of **5** and **13** is not possible at present.

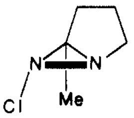

5

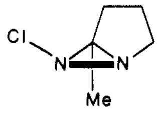

13

Acknowledgment. This work was supported in part by the Natural Sciences and Engineering Research Council of Canada and by a grant from Control Data Corporation (Canada). We thank Supercomputer Services of the University of Calgary for computing time on the CDC Cyber 205.

Excited-State Behavior of Tryptamine and Related Indoles. Remarkably Efficient Intramolecular Proton-Induced Quenching[1]

Haruo Shizuka,*[2a] Manabu Serizawa,[2a] Hirokazu Kobayashi,[2a] Kosei Kameta,[2a] Hiroshi Sugiyama,[2b] Teruo Matsuura,[2b] and Isao Saito*[2b]

Contribution from the Department of Chemistry, Gunma University, Kiryu, Gunma 376, Japan, and the Department of Synthetic Chemistry, Faculty of Engineering, Kyoto University, 606 Kyoto, Japan. *Received May 26, 1987*

Abstract: The excited-state behavior of tryptamine and 1,2,3,4-tetrahydrocarbazoles possessing alkylamino side chains in the absence and presence of 18-crown-6 in $MeOH-H_2O$ (9:1) mixtures has been studied by means of nanosecond single-photon counting, fluorimetry, and photochemical H–D isotope exchange. The fluorescence intensity of these indoles increases significantly with increasing concentration of 18-crown-6. The relatively short lifetime of the tryptamine ammonium ion **1** is not ascribed to external quenching but rather to internal quenching. The rate constant k_q for internal quenching can be estimated from the equation $k_q = \tau_0^{-1} - \tau_{\max}^{-1}$, where τ_0 and $\tau_{\max}$ represent the fluorescence lifetimes for free **1** and the 1:1 **1**–crown ether complex, respectively. Internal quenching originates from electrophilic proton attack by the $-N^+H_3$ (or $-N^+D_3$) group of **1** at the C-4 position of the excited indole ring. For **3** (the tetrahydrocarbazole derivative $R(CH_2)_3N^+H_3$) the k_q value comprises the electrophilic proton attack at the C-8 position plus other quenching (probably charge-transfer quenching) between the excited indole moiety (R^*) and the $-N^+H_3$ (or $-N^+D_3$) group. The stabilization constant K_g for the corresponding ammonium ion and 18-crown-6 can be determined by fluorimetry. The kinetic and thermodynamic parameters for the internal quenching and the complex formation, respectively, have been described.

The mechanistic study on the fluorescence decay of tryptophan (Trp) in polar media is of special interest in photophysics and photobiochemistry.[3,4] A number of mechanisms for the decay process of the excited Trp have been proposed.[3] Two types of quenching mechanisms have been proposed: internal and external as described below. The internal quenching of Trp has been

---

[1] The preliminary work was presented at the Symposium on Photochemistry, Sakai, November, 1986. This work was supported by a Scientific Research Grant-in-Aid of the Ministry of Education, Science and Culture of Japan (no. 61123008). One of the authors (I.S.) is grateful to Ministry of Education, Science and Culture, Grant-in-Aid for Specially Promoted Research (no. 61065003).

[2] (a) Department of Chemistry, Gunma University. (b) Department of Synthetic Chemistry, Kyoto University.

[3] Creed, D. *Photochem. Photobiol.* **1984**, *39*, 537.

[4] Lumry, R.; Hershberger, M. *Photochem. Photobiol.* **1978**, *27*, 819.